Electronic bound states of a two-ion center immersed in high-density plasmas

Philippe Malnoult, Brigitte d'Etat, and Hoe Nguyen
Département de Recherches Physiques, Spectronomie des Gaz et des Plasmas, Université Pierre et Marie Curie, Tour 22, 75252 Paris CEDEX 05, France
and Laboratoire pour l'Utilisation des Lasers Intenses, Ecole Polytechnique, 91120 Palaiseau, France
(Received 29 November 1988; revised manuscript received 21 February 1989)

In order to evaluate the simultaneous influence of a neighboring ion located at an arbitrary distance R and of free electrons on atomic bound states in high-density plasmas ($N_e \gtrsim 10^{23}$ cm^{-3}) we have suggested a transient molecule model that consists of a two-ion center surrounded by bound and free electrons. The Dirichlet boundary condition is laid down in such a way to make the total electrostatic potential constant over the entire molecular envelope and also to obtain the limit of two independent ion spheres or that of one united ion sphere when $R \to \infty$ or $R \to 0$, respectively. A closed form has been obtained for the interaction potential between bound and free electrons at the high-temperature limit. Energy levels and wave functions have been evaluated by diagonalizing the total Hamiltonian in the subspace of the lowest 40 molecular levels. A possible appearance of new spectral components and, in particular, a drastic reduction of the Stark effect are clearly shown.

I. INTRODUCTION

High-density plasmas are of major interest according to the following recent laboratory experiments: inertial confinement fusion with intense laser or ion beams, impact on metal targets using subpicosecond laser pulses, selective laser ionization of alkali vapors, laser excitation of cryogenic hydrogen, and various pinch techniques. In these plasmas the Coulomb interactions between particles can largely exceed their thermal energy.[1] Therefore the treatment of the most important problems,[2] such as electron transport, stopping power, equation of state, and line broadening, relies on the knowledge of atomic structures and related interaction processes. Until now, the ion-sphere model has been commonly used: each atom consists of a nuclear charge Ze located at the center of a spherical cavity with radius $R_0=[3(Z-k)/4\pi N_e]^{1/3}$ where N_e is the volume-averaged electron density and k denotes the number of bound electrons. Inside the ion sphere the density number ρ_e of free electrons, which ensure the overall electrical neutrality, is assumed constant or, more precisely, calculated by means of a self-consistent-field method. Outside the ion sphere the plasma is approximately replaced by neutralizing uniform distributions of electrons and ions. Detailed data have been given for hydrogenlike[3-5] ($k=1$) and heliumlike[6] ($k=2$) systems. The most useful and timely improvement to be brought into the previous atomic model concerns the influence of neighboring ions. Indeed, in calculating the electronic pressure or the ionization state in dense and hot plasmas, for example, we have to distinguish whether the outermost atomic bound states hybridize into propagating waves or molecular bound states. In line-broadening theory for moderate-density plasmas,[7] it has been shown that the nearest-neighbor ion effect occurs principally through the dipolar and quadrupolar term of the multipolar expansion. In particular, the quadrupolar term allows one to explain the strong asymmetry[8-10] observed in hydrogenlike lines and also to foresee a large change[11] in some heliumlike profiles. To explain effects occurring in very far line wings, such as satellite intensity and shape,[12,13] the previous multipolar expansion must be replaced by an exact molecular calculation. In high-density plasmas this molecular calculation is imperative because the mean distance between ions and the atomic radii of interest are often of the same order of magnitude.

In this paper we are interested in electronic bound states of a *two-ion center* which consists of a few number k of bound electrons and two ions separated by an arbitrary internuclear distance R and embedded in dense plasmas. Principally, we shall consider the numbers of charge, electron temperatures, and densities of respective orders of magnitude of 10 and 100 eV and 10^{23} cm^{-3} which characterize the most dense zone of plasmas currently created by focusing high-power laser beams on planar or spherical targets.

Section II is devoted to defining the electrostatic boundary conditions on the above-mentioned physical system. A detailed calculation of the potential created by a homogeneous plasma is given there too. Principal effects of this potential on electronic bound states of a two-ion center and their incidence on line-broadening aspect are considered in Sec. III.

II. FREE-ELECTRON POTENTIAL IN PLASMA

We consider a molecular volume $\mathcal{V}$ which encloses k bound electrons and many ions with charge number Z_i ($i=1,2,\ldots$), fixed in a given spatial configuration. In addition, this physical system involves $Z_{\text{eff}}=\sum_i Z_i - k$ free electrons ensuring overall electrical neutrality. Outside the molecular volume, we assume that the plasma could be replaced by neutralizing uniform distributions

due to electrons and ions which lead to a constant electrostatic potential conventionally taken to be zero. Denoting by $-e$ the electron elementary charge and by ρ_e the number density of free electrons, the electrostatic potential V_e due to the latter satisfies the Poisson equation:

$$\Delta V_e = 4\pi e \rho_e \ . \tag{1}$$

Here the Laplacian Δ and the number density ρ_e ought to be expressed in a suitable coordinate system according to the symmetry of ionic configuration.

In spherical symmetry, valid for ionic monocenter systems, we recall[3] that the electrostatic potential V_e is given by

$$V_e(r) = -4\pi e \left[\frac{1}{r} \int_0^r r' + \int_r^{R_0} \right] r' \rho_e(r') dr' \ , \tag{2}$$

where the "ionic radius" R_0 is defined by the Dirichlet boundary condition:

$$V_e(R_0) + \frac{Z_{\text{eff}} e}{R_0} = 0 \ . \tag{3}$$

Here, $Z_{\text{eff}} e$ is the effective ionic central charge taking into account the screening effect due to bound electrons.

By using Eq. (2) and introducing the volume-averaged electron density:

$$N_e = \frac{3}{R_0^3} \int_0^{R_0} \rho_e(r) r^2 dr \ , \tag{4}$$

and the mean distance between electrons defined by $4\pi N_e r_e^3/3 = 1$, the boundary condition, Eq. (3), is equivalent to

$$R_0 = \left[\frac{3 Z_{\text{eff}}}{4\pi N_e} \right]^{1/3} = r_e Z_{\text{eff}}^{1/3} \ . \tag{5}$$

We note that this boundary condition coincides with the electrical neutrality one: $4\pi N_e/3 = Z_{\text{eff}}$. This is not true for a more general ionic configuration. In the case of a uniform electron gas, $\rho_e(r) = N_e$, Eq. (2) can be written as

$$V_e(r) = -\frac{e}{2r_e^3}(3R_0^2 - r^2) \ . \tag{6}$$

In the right-hand side of Eq. (6), the first term $-3eR_0^2/2r_e^3 = -3Z_{\text{eff}}^{2/3} e/2r_e$ is the ionization potential lowering due to electron pressure, while the second term $er^2/2r_e^3$ gives rise to spectral line shifts.

A. Molecular model for transient two-ion centers in plasmas

In the following, we consider the more general case of two ionic centers with charge number Z_1 and Z_2, separated by a given distance R (Fig. 1). In terms of the elliptic coordinates:

$$\lambda = \frac{r_1 + r_2}{R} \in [1, \infty[\ ,$$

$$\mu = \frac{r_1 - r_2}{R} \in [-1, +1] \ ,$$

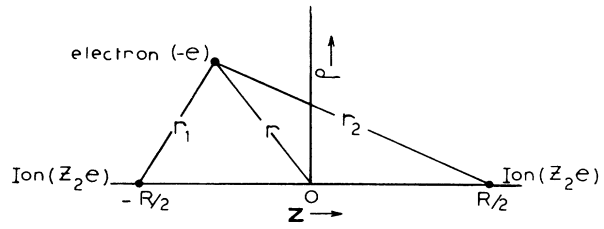

FIG. 1. Relative position of a bound electron and two fixed ions in a two-ion center.

the Poisson equation, Eq. (1), becomes

$$\left[\frac{\partial}{\partial\lambda}(\lambda^2 - 1)\frac{\partial}{\partial\lambda} + \frac{\partial}{\partial\mu}(1 - \mu^2)\frac{\partial}{\partial\mu} \right] V_e(\lambda,\mu) = \pi e R^2 (\lambda^2 - \mu^2) \rho_e(\lambda,\mu) \ . \tag{7}$$

In order to specify the Dirichlet boundary condition for this equation, we suggest choosing as a molecular envelope, the ionic equipotential surface which satisfies the electrical neutrality condition. This choice is probably the most physical one because it refers directly to the ionization potential lowering and also, as it will be shown later, it allows us to retrieve the suitable limit cases, namely, the case of two separated independent ion spheres for $R \to \infty$ and that of the united doubly charged ion sphere for $R \to 0$.

For a homonuclear system ($Z_1 = Z_2 = Z$) for example, the ionic potential is

$$V_i = Ze \left[\frac{1}{r_1} + \frac{1}{r_2} \right] = V_s \frac{\lambda}{\lambda^2 - \mu^2} \ , \tag{8}$$

where $V_s = 4Ze/R$ is the potential value at the singular point O.

The molecular envelope is then defined by

$$\lambda = \lambda(u,\mu) = \tfrac{1}{2}[u + (u^2 + 4\mu^2)^{1/2}] \ , \tag{9}$$

where the parameter $u = V_s/V_i$ is smaller or larger than unity according to whether the equipotential surface encloses two separated volumes or a united one, respectively. The value of u is deduced from the electrical neutrality condition:

$$Z_{\text{eff}} = \int d\mathcal{V} \rho_e(\lambda,\mu) = N_e \mathcal{V} \ , \tag{10}$$

where we recall that Z_{eff} and N_e are the effective total ion charge and the volume-averaged electron density, respectively. In terms of the elliptic coordinates, we note that the elementary volume is

$$d\mathcal{V} = 2\pi (R/2)^3 (\lambda^2 - \mu^2) d\mu \, d\lambda \ ,$$

and that the integration domain is defined by

$$\lambda \in [1, \lambda(u,\mu)] \ ,$$

$$\mu \in [-1, 1] \quad \text{for } u > 1 \ ,$$

and

$$\mu\in[-1,-(1-u)^{1/2}]\cup[(1-u)^{1/2},1] \quad \text{for } u<1 \ .$$

The molecule volume is then

$$\mathcal{V}=\frac{4\pi}{3}\left[\frac{Ru}{2}\right]^3 I(u) \ , \tag{11}$$

where, for $u \geq 1$:

$$I(u)=\frac{1}{4u^2}\left[2u^2+\left[\frac{7u^2}{8}-1\right]\left[1+\frac{4}{u^2}\right]^{1/2}+\frac{9u^3}{32}\ln\frac{(1+u^2/4)^{1/2}+1}{(1+u^2/4)^{1/2}-1}\right]=1-\frac{3}{5u^4}+O\left[\frac{1}{u^6}\right] , \tag{12}$$

and for $u \leq 1$:

$$I(u)=\frac{1}{2u^2}\left[u^2+\frac{(1-u)^{1/2}}{u}(1+u/2-3u^2/8-9u^3/16)-\frac{1}{u}(1+u^2/4)^{1/2}(1-7u^2/8)+\frac{9u^3}{32}\ln\frac{(1+u^2/4)^{1/2}+1}{1+(1-u)^{1/2}-u/2}\right]$$
$$=\frac{1}{4}\left[1+\frac{3u}{4}+\frac{3u^2}{8}+O(u^3)\right] . \tag{13}$$

Taking into account Eqs. (10) and (11), the suitable parameter u for the molecular envelope, Eq. (9), is given by

$$u^3 I(u)=q^3 \ , \tag{14}$$

where

$$q=\frac{2r_e}{R}Z_{\text{eff}}^{1/3} \ . \tag{15}$$

Since $r_e Z_{\text{eff}}^{1/3}$ and $R/2$ are the ion-sphere radius and half the internuclear distance, respectively, we can see that a large value of q corresponds to an important hybridization of atomic wave functions into molecular ones. Also, we note that its smallest value for having a continuous volume which encloses the two ions is obtained with $u=1$, i.e., according to Eqs. (13) and (14):

$$q_0=[I(1)]^{1/3}=\left[\frac{1}{2}\left[1-\frac{\sqrt{5}}{16}+\frac{9}{32}\ln(\sqrt{5}+2)\right]\right]^{1/3}$$
$$=0.858\,681 \ . \tag{16}$$

As we are interested in spectra of given k bound electrons, the effective charge number to be used in Eq. (15) is $Z_{\text{eff}}=2Z-k$ or $Z_{\text{eff}}=2(Z-k)$ according to $q>q_0$ or $q<q_0$, respectively.

In the following, we often use $q/u(q)$ instead of $u=u(q)$. Numerical calculations show that Eq. (14) can be expressed in a more explicit form as

$$\frac{q}{u(q)}=\begin{cases}\dfrac{1}{2^{2/3}}\left[1+\dfrac{2^{2/3}q}{4}+\dfrac{(2^{2/3}q)^3}{113.55}\right] & \text{for } q<q_0 \\ \dfrac{q^6+0.07}{q^2(q^4+0.20)} & \text{for } q>q_0 \ .\end{cases} \tag{17}$$

Equations (8)–(17) can be generalized to systems with $Z_1 \neq Z_2$ without any extra difficulty.[14]

B. Free-electron potential inside the molecular volume

Going back to the Poisson equation, Eq. (7), we note that the number density of free electrons $\rho_e(\lambda,\mu)$ is generally given by suitable statistics involving the local temperature in plasmas and the local total electrostatic potential which results from ions, free and bound electrons. Therefore Eq. (7) is a nonlinear differential equation, closely coupled to the Schrödinger equation for bound electrons. To solve it, we have to use self-consistent-field methods which are expensive in computational time, especially when we are concerned with nonseparable coordinates. In this paper, we propose to consider a uniform electron gas (UEG), i.e., to use Eq. (7) with $\rho_e(\lambda,\mu)$ replaced by N_e. This study is useful for the following three reasons.

Firstly, the UEG model is valid for very-high-temperature plasmas[3,4] where the kinetic energy of free electrons is larger than their potential energy. It is also valid for current temperatures in laser plasmas when we are interested in describing highly excited atomic states.[3,6] For $T_e=500$ eV for example, curve (a) in Fig. 1 of Ref. 3 shows that only atomic states with $n=1,2$ are located in the internal region with a large density gradient and really require an accurate self-consistent-field calculation.

Secondly, with the assumption $\rho_e(\lambda,\mu)\simeq N_e$, the electrostatic potential V_e can be obtained in a closed form which shows tendencies of atomic parameters varying with N_e and R. In particular, as it can be seen in Eq. (19), this closed form allows us to retrieve the appropriate ion-sphere models for $R\rightarrow 0$ and $R\rightarrow\infty$.

Thirdly, as already pointed out in Ref. 3, the interaction potential and atomic data deduced from the UEG model can serve as suitable initial conditions in iterative processes occurring in a more complete self-consistent-field calculation.

By replacing $\rho_e(\lambda,\mu)$ by N_e, Eq. (7) becomes

$$\left[\frac{\partial}{\partial\lambda}(\lambda^2-1)\frac{\partial}{\partial\lambda}+\frac{\partial}{\partial\mu}(1-\mu^2)\frac{\partial}{\partial\mu}\right]V_e=\pi eR^2N_e(\lambda^2-\mu^2)$$
$$=\frac{3eR^2}{4r_e^3}(\lambda^2-\mu^2) \ . \tag{18}$$

The invariance of this equation with respect to changing μ into $-\mu$ shows that the potential depends on $|\mu|$ and not μ. In addition, we can easily verify that $(eR^2/8r_e^3)(\lambda^2+\mu^2)$ is a particular solution of Eq. (18). Therefore the general solution can be written as

$$V_e(\lambda,|\mu|)=\frac{eR^2}{4r_e^3}\left[\frac{\lambda^2+\mu^2}{2}-L(\lambda,|\mu|)\right], \tag{19}$$

where $L(\lambda,|\mu|)$ is solution of the Laplace equation, i.e., Eq. (18) with the right-hand-side member replaced by zero. Now, to complete the definition of V_e we have to introduce the Dirichlet boundary condition. As already pointed out at the beginning of Sec. II, the latter turns into canceling the total electrostatic potential:

$$V_T(\lambda,|\mu|)=\frac{2eZ_{\text{eff}}}{R}\left[\frac{\lambda}{\lambda^2-\mu^2}+\frac{1}{q^3}\left[\frac{\lambda^2+\mu^2}{2}-L(\lambda,|\mu|)\right]\right], \tag{20}$$

over the entire molecular envelope. We recall that the latter and the parameter q are defined by Eqs. (9) and (15), respectively. We verify easily that $V_T(\lambda(u,\mu),|\mu|)=0$ is equivalent to

$$L(\lambda(u,\mu),|\mu|)=q^2\left[\frac{q}{u}+\frac{u^2}{2q^2}\right]+\mu^2\left[1+\frac{u}{u+(u^2+4\mu^2)^{1/2}}\right]. \tag{21}$$

Since the Laplace solution $L(\lambda,|\mu|)$ can be expanded as a linear combination of Legendre polynomial products $P_n(\lambda)P_n(|\mu|)$, it is useful to write the limiting behaviors of the second member in Eq. (21) as

$$L(\lambda(u),|\mu|)=\begin{cases}\lambda(u,\mu)|\mu|+\dfrac{3.2^{1/3}}{4}q^2+O(q^3)\\ \dfrac{3}{2}q^2+\dfrac{1}{2}+\dfrac{2}{3q^2}P_2(\lambda(u,\mu))P_2(\mu)+O\left[\dfrac{1}{q^2}\right].\end{cases} \tag{22}$$

For $q=2^{4/3}(Z-k)^{1/3}r_e/R \ll q_0$, by approximating $L(\lambda,|\mu|)$ to $\lambda|\mu|+3.2^{1/3}q^2/4$, Eq. (19) becomes

$$V_e=-\frac{e}{2r_e^3}\left[3[r_e(Z-k)^{1/3}]^2-\left[\frac{R(\lambda-|\mu|}{2}\right]^2\right]. \tag{23}$$

This agrees with Eq. (6) if R_0 and r are taken to be $r_e(Z-k)^{1/3}$ and $R(\lambda-|\mu|/2)=\min(r_1,r_2)$ respectively. Here, $\min(r_1,r_2)$ denotes the smallest of the distances between a given bound-electron position and the two ionic centers. So, our model leads to independent ion-sphere potentials centered at one of the ionic centers when the internuclear distance is large enough.

Likewise, for $q=2(2Z-k)^{1/3}r_e/R \gg q_0$, according to Eqs. (22) and (19), we have $L(\lambda,|\mu|)\simeq\frac{3}{2}q^2+\frac{1}{2}$ and

$$V_e=-\frac{e}{2r_e^3}\{3[(2Z-k)^{1/3}r_e]^2-\tfrac{1}{4}R^2(\lambda^2+\mu^2-1)\}, \tag{24}$$

respectively. Here, we recognize again the potential in the ion-sphere model, Eq. (6), where, however, we have to take

$$R_0=r_e(2Z-k)^{1/3},$$

corresponding to a shielded double charge $Z_{\text{eff}}=2Z-k$ and

$$r^2=\tfrac{1}{4}R^2(\lambda^2+\mu^2-1).$$

Between the limiting behaviors defined by Eqs. (23) and (24), we can achieve the electrostatic potential due to free electrons by writing the Laplace solution in Eq. (19) as

$$L(\lambda,\mu)=q^2\left[\frac{q}{u}+\frac{u^2}{2q^2}\right]+\sum_{n(\geq 0)}a_nP_n(\lambda)P_n(|\mu|), \tag{25}$$

where coefficients a_n are determined by means of the Dirichlet boundary condition, namely, according to Eq. (21):

$$\sum_{n(\geq 0)}a_nP_n[\lambda(u,\mu)]P_n(|\mu|)=\mu^2\left[1+\frac{u}{u+(u^2+4\mu^2)^{1/2}}\right]. \tag{26}$$

In Eqs. (25) and (26) we recall that u depends on the hybridization parameter q according to the electrical neutrality condition, Eq. (14) or (17). Besides, we note that the number of terms retained in the sum $\sum_{n(\geq 0)}$ must be large enough to ensure the Dirichlet condition accurately over the entire molecular envelope [i.e., for all $|\mu|$ in Eq. (26)] and also to include the most significant multipolar interactions. The coefficients a_n with $n \leq N$ have been calculated by writing Eq. (26) for $N+1$ suitably chosen values of $|\mu|$ and by solving the subsequent linear equation system. It is found that $N=4$ is a convenient choice. Indeed, as shown in Fig. 2, only a_n with $n \leq 3$ are numerically appreciable. We note that $a_0=\frac{1}{2}$ for $q \gg q_0$ and $a_1=1$ for $q \ll q_0$ in good agreement with limiting expansions in Eq. (22).

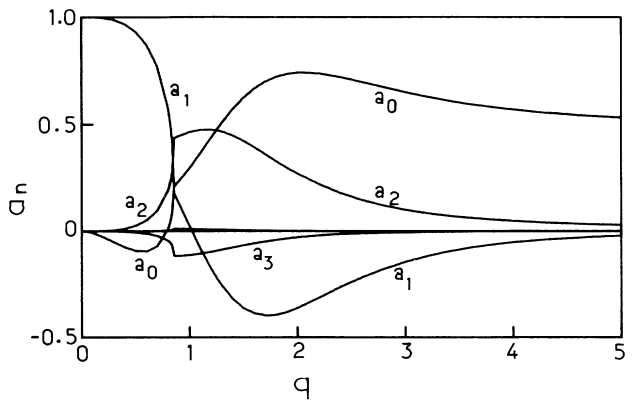

FIG. 2. Expansion coefficients of the Laplace potential as functions of the hybridization parameter $q=2r_eZ_{\text{eff}}^{1/3}/R$ [see Eqs. (15), (19), and (26) in the text].

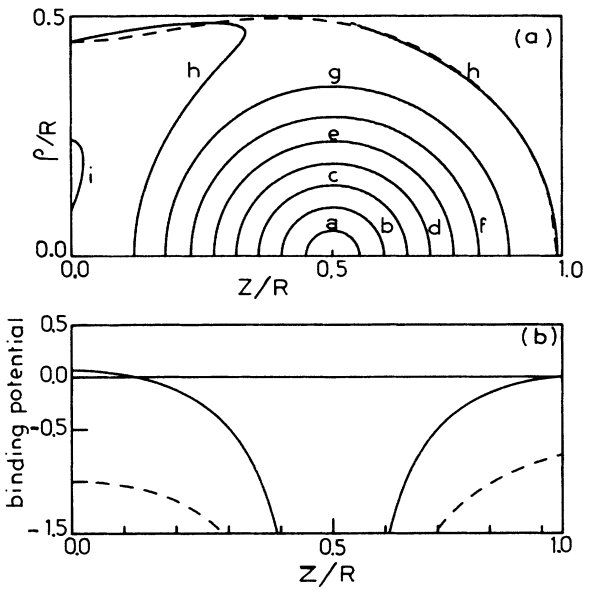

FIG. 3. (a) Meridian lines of equipotential surfaces relative to the total potential V_T with $q=2^{1/3}$ [see Eq. (20) in the text]. The assigned letters a, b, c, d, e, f, g, h, and i correspond, respectively, to the values 3.9, 1.7, 0.96, 0.58, 0.35, 0.2, 0.09, 0.0, and -0.07 for the total potential in units of $2eZ_{\text{eff}}/R$. We note that the envelope line (dashed curve) coincides accurately with the zero potential meridian line (curve h). (b) Binding potential due to ions only V_i (— — —) and to ions and free electrons V_i+V_e (——) measured in units of $2eZ_{\text{eff}}/R$ ($Z=10$, $Z_{\text{eff}}=2Z-1=19$, $q=2^{1/3}$, $N_e=2\times10^{23}$ cm^{-3}). We point out that midway between the nuclei the barrier potential is positive wherever the total potential is negative [region limited by curve h and enclosing curve i in Fig. 3(a)].

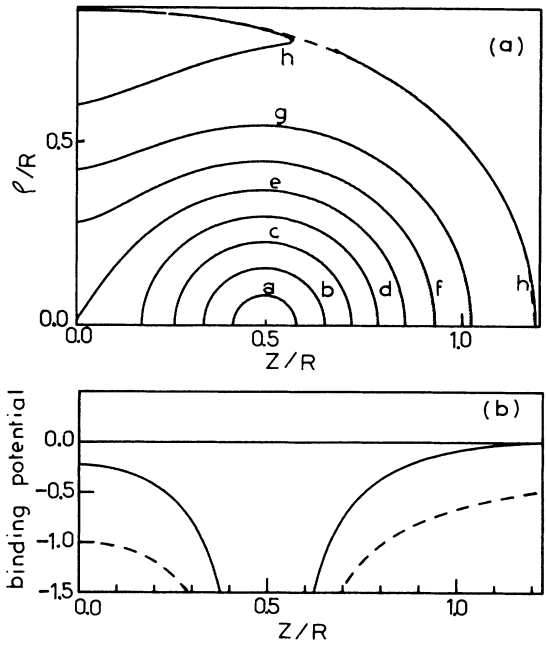

FIG. 4. (a) Meridian lines of equipotential surfaces relative to the total potential V_T with $q=2$ [see Eq. (20) in the text]. The assigned letters a, b, c, d, e, f, g, and h correspond, respectively, to the values 2.4, 1.1, 0.6, 0.37, 0.22, 0.13, 0.06, and 0.0 for the total potential in units of $2eZ_{\text{eff}}/R$. (b) Binding potential due to ions only V_i (— — —) and to ions and free electrons V_i+V_e (——) measured in units of $2eZ_{\text{eff}}/R$ ($Z=10$, $Z_{\text{eff}}=2Z-1=19$, $q=2$, $N_e=2\times10^{23}$ cm^{-3}). We point out that midway between the nuclei the barrier potential is clearly below the ionization limit.

To give a general idea about plasma effects on electronic bound states, in Figs. 3(a) and 4(a) we show meridian lines of equipotential surfaces relative to the total electrostatic potential, Eq. (20). We can see that the latter is zero over the boundary line, as it should be.

With $q=2^{1/3}$, i.e., $R\simeq 2r_eZ^{1/3}$, Fig. 3(a) corresponds approximately to a configuration where two ion spheres with radius $r_eZ^{1/3}$ are in contact. We note that equipotential surfaces with positive potential are nearly spherical and enclose only one of the two ionic sites. In addition, midway between the latter there is a wide region where negative values of the total potential show that the ions are indeed completely screened by free electrons. Therefore the two ions with their surrounding electrons are actually separated from each other and can be treated in the framework of previous monocenter theories.[3,6] This idea is reinforced by examining Fig. 3(b), which clearly shows a positive potential barrier in the middle of the internuclear axis. For the purpose of comparison, the binding potential due to the ions only is given in the same figure. We note that one of the free-electron effects consists of an important continuum lowering and points to a drastic reduction of bound-state number.

With $q=2$, i.e., $R\simeq 1.26r_eZ^{1/3}$, Figs. 4(a) and 4(b) correspond to configurations where the two ion spheres start to penetrate each other. In Fig. 4(a) we note that most of the equipotential surfaces have no spherical symmetry and enclose the two ions together. Furthermore, the latter are not completely screened from each other by free electrons owing to the disappearance of the negative potential region. In addition to presenting the same continuum lowering as in Fig. 3(b), Fig. 4(b) shows a potential barrier for negative potential values. This fact and the two-ion center behavior of equipotential surfaces in Fig. 4(a) point to a hybridization of atomic wave functions towards molecular ones.

III. ELECTRONIC BOUND STATES OF A TWO-ION CENTER IMMERSED IN PLASMAS

This section is devoted to the study of electronic bound states, as quantum-mechanical solutions of the wave equation:

$$(H_0-eV_e)|\psi\rangle=W|\psi\rangle\ , \tag{27}$$

where V_e is the electrostatic potential due to free electrons, Eq. (19), and W denotes the electronic energy, i.e., the difference between the total molecular energy and the nuclear Coulomb term $Z_1Z_2e^2/R$. In Eq. (27) H_0 is the Hamiltonian of the diatomic molecule free from plasma effects. For one-bound-electron systems we have

$$H_0=\frac{p^2}{2m}-e^2\left[\frac{Z_1}{r_1}+\frac{Z_2}{r_2}\right]\ , \tag{28}$$

or, in terms of elliptic coordinates:

$$H_0=-\frac{2a_0e^2}{R^2(\lambda^2-\mu^2)}\left[\left[\frac{\partial}{\partial\lambda}(\lambda^2-1)\frac{\partial}{\partial\lambda}+\frac{1}{\lambda^2-1}\frac{\partial^2}{\partial\Phi^2}+\frac{R}{a_0}(Z_1+Z_2)\lambda\right]+\left[\frac{\partial}{\partial\mu}(1-\mu^2)\frac{\partial}{\partial\mu}+\frac{1}{1-\mu^2}\frac{\partial^2}{\partial\Phi^2}-\frac{R}{a_0}(Z_1-Z_2)\mu\right]\right] . \tag{29}$$

According to the discussion given about Figs. 3(a) and 3(b) we know that our present model leads to new aspects only for $q\gtrsim 2^{1/3}$, i.e., when the two ionic sites are enclosed in a continuous molecular volume. Therefore it is reasonable to consider the bound electron in its molecular states instead of the atomic ones, more or less perturbed by the nearest-neighbor ion. Owing to the interaction potential $-eV_e$, Eq. (27) is not separable, even in the elliptic coordinate system (λ,μ,Φ). In this paper, we suggest using the truncated diagonalization method where the wave functions $\psi(\lambda,\mu,\Phi)$ are expanded in terms of the eigenfunctions of H_0, Eq. (28) or (29):

$$\psi(\lambda,\mu,\Phi)=\sum_k b_k\psi_k^0(\lambda,\mu,\Phi) . \tag{30}$$

Henceforth, we shall use the spherical quantum number set (N,L,m) or the parabolic one (n_1,n_2,m) (with $n_1+n_2+|m|+1=n$) to characterize an electronic state of united atom $(R\to 0)$ or moderately separated atom $(0<R<2R_0)$, respectively. The relations[15] between these quantum numbers are deduced from the conservation of the number of nodal surfaces of the eigenfunction of a state as R is varied. Besides, it will be shown that the ion field is completely screened by free electrons for $R\gtrsim 2R_0$; then the spherical quantum number set (n,l,m) will be used to characterize this asymptotic behavior.

A. General consideration on an isolated one-electron diatomic molecule

By setting[15]

$$\psi^0(\lambda,\mu,\Phi)=L(\lambda)M(\mu)e^{im\Phi} , \tag{31}$$

where m is the magnetic quantum number, the Schrödinger equation $H_0|\psi^0\rangle=W^0|\psi^0\rangle$ separates out into the following "inner" and "outer" coupled equations:

$$\left[\frac{\partial}{\partial\mu}(1-\mu^2)\frac{\partial}{\partial\mu}+\left[-\frac{m^2}{1-\mu^2}-2kp\mu-p^2(1-\mu^2)+C_\mu\right]\right]M(\mu)=0 , \tag{32a}$$

$$\left[\frac{\partial}{\partial\lambda}(\lambda^2-1)\frac{\partial}{\partial\lambda}+\left[-\frac{m^2}{\lambda^2-1}+2p(\sigma+m+1)\lambda-p^2(\lambda^2-1)-C_\lambda\right]\right]L(\lambda)=0 , \tag{32b}$$

where C is the separation constant and

$$p^2=-\frac{R^2W^0(R)}{2},\quad z=\frac{4Z_1Z_2}{(Z_1+Z_2)^2} ,$$

$$k=\frac{R(Z_1-Z_2)}{2p},\quad r=R(Z_1,Z_2) ,$$

$$\sigma+|m|+1=\frac{R(Z_1+Z_2)}{2p},\quad k^2=(1-z)(\sigma+|m|+1) .$$

We note that $M(\mu)$ and $L(\lambda)$ are square-integrable solutions only if the separation constant C coincides with an eigenvalue $C_\mu(p,k)$ of Eq. (32a) and an eigenvalue $C_\lambda(\sigma,k)$ of Eq. (32b), respectively. We have then

$$C_\mu(p,k)=C_\lambda(\sigma,k) , \tag{33}$$

which allows us to express electronic bound energies W^0 in terms of R, Z_1, Z_2, and $|m|$.

Writing

$$M(\mu)=e^{p\mu}\sum_l g_l P_l^m(\mu) , \tag{34a}$$

where P_l^m is the associated Legendre polynomial of the first kind and writing

$$L(\lambda)=(\lambda^2-1)^{m/2}+(\lambda+1)^\sigma e^{-p\lambda}\sum_l f_l\left[\frac{\lambda-1}{\lambda+1}\right]^l , \tag{34b}$$

Eqs. (32a) and (32b) turn into three-term recurrence relations for g_l and f_l, respectively. By using the perturbation treatment at small internuclear distance we obtain for the ground state, i.e., with the principal quantum number of united atom $N=1$:

$$W^0_{100}(\text{in a.u.})=-\frac{(Z_1+Z_2)^2}{2}\left\{1-\frac{1}{3}zr^2\left[1-r+\frac{3}{5}\left[1-\frac{16}{27}z\right]r^2-\frac{1}{15}\left[4-\frac{199+30\rho}{12}z\right]r^3\right]+O(r^6)\right\} , \tag{35}$$

TABLE I. Expansion coefficients $\varepsilon_k(N,L,m)$ of the energy levels W^0_{NLm} ($N=2$; L; $|m|=0$ or 1) for short internuclear distances R [see Eq. (36) in the text].

ε_k \ (N,L,m)	(2,0,0)	(2,1,0)	(2,1,±1)
ε_0	1	1	1
ε_1	0	0	0
ε_2	$-z/6$	$+z/30$	$-z/60$
ε_3	$+z/6$	0	0
ε_4	$-\left[\frac{216-83z}{2^4 3^5 5}\right]z$	$z\left[\frac{-1350+1769z}{2^4 3^3 5^3 7}\right]$	$\frac{z}{60}\left[\frac{-2700+284z}{25200}\right]$
ε_5	$-\left[\frac{(496+60\rho)z-177}{2^5 3^3 5}\right]z$	$-\frac{z}{30}\left[\frac{15+4(\rho-\frac{1}{2})z}{120}\right]$	$-\frac{z}{60}\left[\frac{15-z(\rho-\frac{1}{2})}{360}\right]$

where

$$r=R(Z_1+Z_2)\ ,$$

$$z=\frac{4Z_1Z_2}{(Z_1+Z_2)^2}\ ,$$

$$\rho=2\exp(2r)E_1(2r)$$

$$\simeq 2\left[-\gamma+\ln\frac{1}{2r}\right]\quad(\gamma=0.577)\ ,$$

and for the first excited states with $N=2$:

$$W^0_{NLm}=-\frac{(Z_1+Z_2)^2}{8}\left[\sum_{k=0}^{5}\varepsilon_k(NLm)r^k+O(r^6)\right]\ , \quad (36)$$

where $N=2$, L, $|m|=0$ or 1, and coefficients ε_k are given in Table I. Equation (35) is in agreement with Brown and Steiner's results,[16] while Eq. (36) is a new one.

For large internuclear distance we can conveniently use the asymptotic expansion in $1/R$ already given in the literature.[8,15,17,18] For intermediate values of R we have solved the above-mentioned three-term recurrence equations by means of continued-fraction calculations. The latter are proved accurate apart from the neighborhood of poles where we have solved Eqs. (32a) and (32b) directly by using Cooley's numerical method.[19] The transition energy between the fundamental level ($1s\sigma g$ or $2p\sigma u$) and the lowest 18 levels is given in Tables II and III (where the unperturbed transition energy of Ne X Lyman-α and Ne X Lyman-β emissions, respectively, are used as reference energy). Each transition is identified by the upper-state Stark quantum numbers (n_1,n_2,m) of the corresponding separated atom. For $Z_1=Z_2$, the letter g

TABLE II. Transition energy $W_{n_1n_2m\,g,u}-W_{000\,u,g}$ measured in a.u. from the unperturbed Lyman transition energy $Z^2(1-1/n^2)/2$ with $Z=10$. For each internuclear distance R and each transition specified by the upper-state quantum number set (n_1,n_2,m) g or u, the value in the top line refers to an isolated two-ion center, while that in the lower line corresponds to a two-ion center immersed in a uniform electron gas with density $N_e=2\times10^{23}$ cm^{-3}. The transitions considered in this table are related to the Stark pattern of Ne X Lyman-α line ($n=2$). In terms of united-atom quantum number sets (N,L,m) the lower states (000) u and g correspond to $(2p\sigma)$ u and $(1s\sigma)g$, respectively, while the upper states listed from the top to the bottom in Table II correspond to $(2p\pi)$ u, $(3d\pi)$ g, $(3d\sigma)$ g, $(4f\sigma)$ u, $(2s\sigma)$ g, $(3p\sigma)$ u, respectively.

(n_1,n_2,m) \ R (units of a_0) / q	7.0 1.53	6.0 1.78	5.0 2.14	4.2 2.55	3.8 2.82	3.4 3.15	3.0 3.57
(0,0,1)u	0.001 44	0.002 20	0.003 60	0.005 69	0.007 33	0.009 59	0.012 48
	−0.016 07	−0.014 89	−0.012 74	−0.009 77	−0.007 57	−0.004 66	−0.000 94
(0,0,1)g	0.001 44	0.002 20	0.003 60	0.005 69	0.007 36	0.009 77	0.013 55
	−0.016 07	−0.014 89	−0.012 74	−0.009 77	−0.007 55	−0.004 50	0.000 05
(1,0,0)g	−0.063 42	−0.086 98	−0.126 70	−0.182 33	−0.225 51	−0.287 62	−0.385 48
	−0.027 67	−0.045 70	−0.084 09	−0.141 79	−0.187 04	−0.251 82	−0.352 69
(1,0,0)u	−0.063 42	−0.086 98	−0.126 70	−0.182 16	−0.224 63	−0.283 12	−0.363 66
	−0.027 05	−0.045 70	−0.084 10	−0.141 66	−0.186 26	−0.247 58	−0.331 71
(0,1,0)g	0.059 23	0.080 11	0.114 33	0.160 32	0.194 46	0.240 73	0.305 65
	−0.012 90	0.002 94	0.036 44	0.085 33	0.122 17	0.172 03	0.241 42
(0,1,0)u	0.059 23	0.080 11	0.114 33	0.160 32	0.194 46	0.240 74	0.305 69
	−0.012 36	0.002 94	0.036 44	0.085 33	0.122 17	0.172 04	0.241 46

TABLE III. Same as Table II except that the considered transitions are related to the Stark pattern of Ne X Lyman-β line ($n=3$) and that the Stark quantum number sets (n_1,n_2,m) g or u listed from the top to the bottom in Table III are respectively related to the following united-atom quantum number sets: $(3d\delta)$ g, $(4f\delta)$ u, $(4f\pi)$ u, $(5g\pi)$ g, $(5g\sigma)$ g, $(6h\sigma)$ u, $(3p\pi)$ u, $(4d\pi)$ g, $(4d\sigma)$ g, $(5f\sigma)$ u, $(3s\sigma)$ g, $(4p\sigma)$ u.

(n_1,n_2,m) \ R (units of a_0) / q	7.0 1.53	6.0 1.78	5.0 2.14	4.2 2.55	3.8 2.82	3.4 3.15	3.0 3.57
(0,0,2) g	0.007 66	0.011 42	0.017 76	0.024 77	0.027 06	0.024 18	0.007 83
	−0.075 80	−0.069 16	−0.057 58	−0.044 26	−0.037 80	−0.035 50	−0.045 61
(0,0,2) u	0.007 66	0.011 45	0.018 30	0.029 46	0.040 34	0.060 21	0.100 03
	−0.075 80	−0.069 16	−0.057 21	−0.040 35	−0.026 25	−0.003 07	0.039 92
(1,0,1) u	−0.092 29	−0.127 36	−0.192 44	−0.309 55	−0.422 14	−0.595 28	−0.838 56
	−0.112 51	−0.129 09	−0.183 96	−0.294 79	−0.404 45	−0.576 25	−0.821 43
(1,0,1) g	−0.092 23	−0.126 50	−0.181 65	−0.241 08	−0.265 62	−0.267 32	−0.210 81
	−0.112 50	−0.128 54	−0.175 10	−0.233 93	−0.260 83	−0.266 96	−0.216 96
(2,0,0) g	−0.214 05	−0.307 13	−0.507 74	−0.872 79	−1.159 32	−1.510 11	−1.891 39
	−0.141 17	−0.212 19	−0.401 55	−0.765 96	−1.058 89	−1.421 34	−1.818 53
(2,0,0) u	−0.213 315	−0.297 04	−0.419 29	−0.504 73	−0.494 47	−0.385 04	−0.077 80
	−0.140 67	−0.204 16	−0.323 67	−0.421 47	−0.422 62	−0.327 87	−0.038 53
(0,1,1) u	0.090 80	0.122 67	0.174 47	0.243 11	0.293 09	0.359 12	0.447 58
	−0.075 04	−0.055 74	−0.003 66	0.073 19	0.129 94	0.204 65	0.303 90
(0,1,1) g	0.090 80	0.122 67	0.174 51	0.243 55	0.294 52	0.363 66	0.461 63
	−0.075 03	−0.055 72	−0.003 60	0.073 55	0.131 13	0.208 54	0.316 35
(1,1,0) g	0.006 86	0.009 92	0.014 39	0.016 32	0.011 86	−0.004 92	−0.047 76
	−0.106 57	−0.090 77	−0.076 84	−0.066 43	−0.065 40	−0.075 37	−0.110 25
(1,1,0) u	0.006 87	0.009 98	0.015 39	0.024 85	0.035 57	0.057 85	0.107 04
	−0.106 51	−0.090 65	−0.076 02	−0.059 26	−0.044 74	−0.018 82	0.033 68
(0,2,0) g	0.162 66	0.216 88	0.303 50	0.416 45	0.498 18	0.606 56	0.754 54
	−0.074 41	−0.047 29	0.033 12	0.154 08	0.244 07	0.363 63	0.525 79
(0,2,0) u	0.162 66	0.216 88	0.303 50	0.416 47	0.498 25	0.606 81	0.755 43
	−0.074 38	−0.047 28	0.033 12	0.154 10	0.244 13	0.363 83	0.526 55

(gerade) or u (ungerade) allows us to distinguish whether the wave function is symmetric or antisymmetric, respectively. For each internuclear distance R and each radiative transition denoted by (n_1,n_2,m) and g or u, Tables II and III show two values. The upper one refers to a diatomic molecule with $Z_1=Z_2=10$, free from plasma effect. We have verified that it agrees with the one given by Bates *et al.*[15] and Madsen and Peek,[20] the discrepancy being within ± 3 in the last of the five figures quoted.

B. Perturbation due to free electrons in plasmas

To include the effects due to free electrons, we expand wave functions according to Eq. (30), in the subspace of the lowest 40 electronic states which, indeed, correlate at large R to atomic states having principal quantum number $n=1,2,3,4$. This restriction is a suitable one because atomic states with $n\geq 5$ are ionized for electron density $N_e \geq 10^{23}$ cm^{-3}, as shown in Table I of Ref. 3. Then, energy levels and wave functions of a two-ion center immersed in a plasma can be obtained by diagonalizing the matrices deduced from Eq. (27) for different values of R. It is worth recalling that $V_e(\lambda,|\mu|)$, Eq. (19), is invariant with respect to the nuclear exchange and consequently connects only states with the same parity. Then the dimension of the matrices to be diagonalized is reduced from 40 to 20. The Hamiltonian matrix elements have been calculated by using the boundary conditions deduced from those of the Dirichlet problem. Indeed, by canceling the total electrostatic potential in Eq. (20), Eqs. (8) and (19) show that the atomic potential acting upon the bound electron over the entire molecular envelope is $V_{\text{out}}=-e^2(1/r_1+1/r_2)/2$, i.e., the potential resulting from the two ion centers screened by $2Z-1$ internal free electrons. In accordance with the charge equilibrium condition and the potential continuity one we assume that V_{out} is also valid outside the molecular envelope. Owing to the exponential decrease of the wave functions in Eq. (30), the relative contribution of this potential tail is indeed very small. Transition energies with free-electron effects are given in Tables II and III, at the lower place for each radiative transition (n_1,n_2,m) g or u. We note that the difference between values at the upper and lower place resulting from the influence of free electrons is really notable. For the purpose of comparison we consider the transition energy shifts in the ion-sphere model by calculating the diagonal matrix elements of $-eV_e$ where V_e is defined by Eq. (6):

$$\langle nlm|-eV|nlm\rangle=\frac{3eR_0^2}{2r_e^3}-\frac{e^2a_0^2}{4r_e^3Z^2}n^2[5n^2+1-3l(l+1)]\,. \tag{37}$$

In particular, for $Z=10$ and $N_e=2\times10^{23}$ cm^{-3} we have

$$\begin{aligned}
&\hbar\Delta\omega((2,0,0)\rightarrow(1,0,0))=-0.024\,20(-0.024\,26)\,,\\
&\hbar\Delta\omega((2,1,m)\rightarrow(1,0,0))=-0.016\,76(-0.016\,80)\,,\\
&\hbar\Delta\omega((3,0,0)\rightarrow(1,0,0))=-0.126\,62(-0.129\,28)\,,\\
&\hbar\Delta\omega((3,1,m)\rightarrow(1,0,0))=-0.109\,86(-0.112\,19)\,,\\
&\hbar\Delta\omega((3,2,m)\rightarrow(1,0,0))=-0.076\,35(-0.077\,89)\,,
\end{aligned}\tag{38}$$

where, for completeness, we have given in parentheses the corresponding values resulting from an exact numerical resolution of Schrödinger equations.[3] Examination of Table II shows clearly that at large R the transition energies of $(1,0,0)$ g and of $(0,0,1)$ g, $(0,1,0)$ g tend towards $\hbar\Delta\omega((2,0,0)\rightarrow(1,0,0))$ and $\hbar\Delta\omega((2,1,0)\rightarrow(1,0,0))$, respectively. This tendency from Stark symmetry towards spherical symmetry is also very clear if we compare the transition energies of $(2,0,0)$ g, of $(1,0,1)$ g, $(1,1,0)$ g and of $(0,2,0)$ g, $(0,0,2)$ g in Table III with $\hbar\Delta\omega((3,0,0)\rightarrow(1,0,0))$, $\hbar\Delta\omega((3,1,0)\rightarrow(1,0,0))$ and $\hbar\Delta\omega((3,2,0)\rightarrow(1,0,0))$, respectively. Likewise, we have verified that Eq. (37) with Z, n, and l replaced by $2Z$, N, and L is a good approximation for our calculation when $R<a_0/2$. This case is not plotted in Tables II and III in consideration of its very small probability related to nuclear repulsion.

The incidence of the above-mentioned effects on linewidths and shifts can be seen more easily in Figs. 5 and 6, where essentially numerical values of Tables II and III are respectively reported. The asymptotic behaviors defined by the ion-sphere model, Eq. (38), are shown on the right side border of each figure. In Fig. 5 (dashed) curves a_0, b_0, and c_0, which represent the transition energy shifts relative to a two-ion center without free-electron effects, remind us of the well-known Stark pattern of the Lyman-α line: one central component and two nearly symmetrical shifted components.

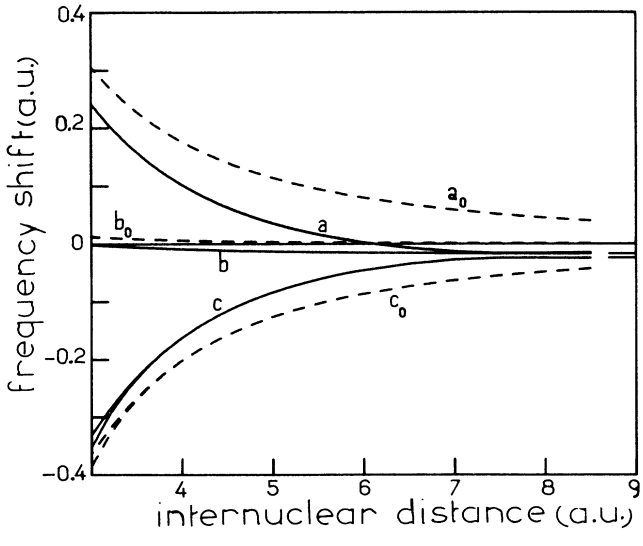

FIG. 5. Frequency shift of Ne X Lyman-α line components as a function of internuclear distance R. Here, we have considered the electron density $N_e=2\times10^{23}$ cm^{-3} and assigned a, b, and c to the radiative transitions with upper states: $(0,1,0)$, $(0,0,1)$, and $(1,0,0)$, respectively. The subscript 0 in a_0, b_0, and c_0 (dashed curves) refers to results where free-electron effects are not taken into account. Likewise the subscript g or u denotes the symmetry of upper states. Indeed, as shown on curves c and c_0, the symmetry splitting occurs only at $R\leq3a_0$.

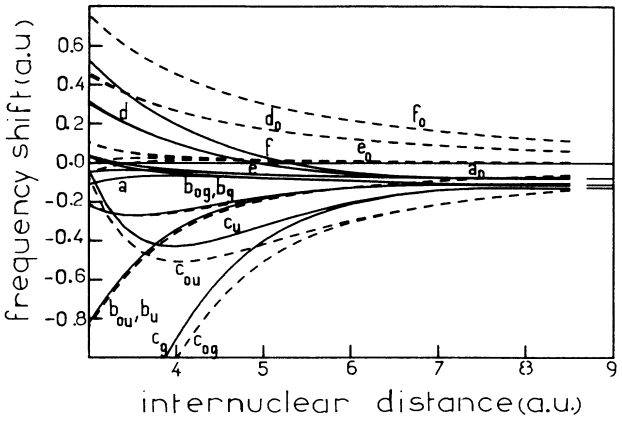

FIG. 6. Frequency shift of Ne X Lyman-β line components as a function of internuclear distance R. Here, the electron density $N_e=2\times10^{23}$ cm^{-3} is considered and the letters a, b, c, d, e, and f refer to the radiative transitions with upper states: $(0,0,2)$, $(1,0,1)$, $(2,0,0)$, $(0,1,1)$, $(1,1,0)$, and $(0,2,0)$, respectively. The meaning of the subscripts $0,g$, and u in $a_{0u,g}\ldots$ is the same as in Fig. 5. As shown by the difference between curves c_u and c_g and between b_u and b_g, we note that the symmetry splitting is appreciable, even at large internuclear distance.

As a first effect of free electrons we point out that at large internuclear distance ($R\gtrsim7a_0$) there are only two really separated transition energies which, in fact, agree with $\hbar\Delta\omega((2,0,0)\rightarrow(1,0,0))$ and $\hbar\Delta\omega((2,1,m)\rightarrow(1,0,0))$. For $R<7a_0$, while states $|2,1,\pm1\rangle$ keep nearly unchanged and constitute the central component a slightly shifted towards a negative value ($=-0.017$ a.u.), states $|2,1,0\rangle$ and $|2,0,0\rangle$ start to be coupled by the ion field and give rise to the shifted components b and c. By comparing the relative positions of the curves in Fig. 5 we can note a second effect of free electrons which consists in reducing the distance between the opposite shifted components. This reduction is about 40% at $R=4a_0$ and increases rapidly when R increases.

The first effect is to be related to the plasma polarization shift already discussed in many recent papers.[3,6,21] The incidence of the second effect lies in the reduction of the Lyman-α linewidth, the importance of which depends on the ion distribution function. Molecular-dynamics calculations[22] performed for laser plasma conditions show that the latter takes appreciable values for the reduced microfield $\beta=(R_0/R)^2\in[0.25,2]$, i.e., for $R/R_0\in[0.71,2]$. Here we have $R_0=4.17a_0$ for the considered electron density ($N_e=2\times10^{23}$ cm^{-3}) and charge state ($Z=10$).

As concerning the components of Lyman-β line plotted

in Fig. 6, we can make the same assertions as previously, namely, the convergence of Stark states towards spherically polarized atomic states for $R \gtrsim 7a_0$ and the reduction of distance between opposite shifted components. In addition, we must, however, point out that there is an important general shift towards negative energy and that curves b_g and c_u [relative to transitions $(1,0,1)$ g and $(2,0,0)$ u, respectively] present a minimum in the neighborhood of $R=3.5a_0$ and $4a_0$, respectively. For the transition $(1,0,1)$ $g \rightarrow (0,0,0)$ u, which is an allowed one as well in the extreme regimes (united and separated atoms) as in the intermediate regime (Stark effect), such a minimum means that a large R interval enclosing $R_m=3.5a_0$ contributes to the intensity at the same frequency $\hbar\Delta\omega=-0.15$ a.u. on the Lyman-β red wing. The corresponding satellite line shape, which is reduced to a Dirac peak in the quasistatic theory, can be obtained from an ion dynamics description where position fluctuations are properly taken into account.

IV. CONCLUSION

With the purpose of evaluating the simultaneous influence of a neighboring ion at arbitrary distance and of free electrons on atomic bound states in dense plasmas, we have suggested a transient molecule model which consists of a two-ion center surrounded by bound and free electrons. The Dirichlet boundary condition is laid down in such a way (a) to make the total potential constant over the entire molecular envelope and the overall number of charge vanishing inside it and (b) to obtain the limit of two independent ion spheres at $R \gg R_0$ ($R_0 \simeq r_e Z^{1/3}$ where r_e is the average distance between electrons) and the limit of a united ion sphere with added charges at $R \ll R_0$. The interaction potential between bound and free electrons has been given in a closed form by assuming a uniform distribution for free electrons. The energy levels related to the atomic principal quantum number $n=1$, 2, and 3 have been calculated with precision by diagonalizing the total Hamiltonian in the subspace of the lowest 40 molecular levels. The results clearly show the following.

(a) For $R \gtrsim 2R_0$, the Stark patterns completely disappear and give way to energy diagrams characteristic of spherically polarized atoms.

(b) For $R < 2R_0$, the free-electron screening effect turns into a drastic reduction of Stark effect. Besides, a new molecular feature becomes apparent by showing several extrema in transition energies.

We can conclude that a molecular treatment including free-electron effects is imperative for electronic bound states in dense plasmas ($N_e \gtrsim 10^{23}$ cm^{-3} for laser plasmas). At the separated atom limit this treatment allows us to retrieve the polarization line shift discussed previously.[3-6,21] For small internuclear distances ($R < 2R_0$), the reduction of Stark effect and the possible excitation of satellite components are new interesting molecular data which should be included in line profile calculations used for diagnosing ultradense plasmas. We intend to extend the present study to nonuniform electron gases and expect to improve it principally for low-lying energy levels in low-temperature plasmas.

ACKNOWLEDGMENTS

We are very grateful to R. M. More for helpful discussions during this work. The efficient technical support from G. Coulaud and J. Grumberg is acknowledged. Département de Recherches Physiques and Laboratoire pour l'Utilisation des Lasers Intenses are Unité Associeé D0071 and Unité Mixte 100 of the Centre National de la Recherche Scientifique, respectively.

[1] M. Baus and J. P. Hansen, Phys. Rep. **59**, 1 (1980).
[2] R. M. More, in *Atomic and Molecular Physics of Controlled Thermonuclear Fusion,* edited by C. Joachain and D. Post (Plenum, New York, 1983), p. 399.
[3] H. Nguyen, M. Koenig, D. Benredjem, M. Caby, and G. Coulaud, Phys. Rev. A **33**, 1279 (1986).
[4] R. Cauble, M. Blaha, and J. Davis, Phys. Rev. A **29**, 3280 (1984).
[5] M. W. C. Dharma-Wardana and F. Perrot, Phys. Rev. A **26**, 2096 (1982).
[6] M. Koenig, Ph. Malnoult, H. Nguyen, Phys. Rev. A **38**, 2089 (1988).
[7] H. R. Griem, *Spectral Line Broadening by Plasmas* (Academic, New York, 1974).
[8] B. d'Etat and H. Nguyen, in *Spectral Line Shapes,* edited by F. Rostas (de Gruyter, Berlin, 1985), Vol. 3, p. 209.
[9] L. A. Woltz and C. F. Hooper, Jr., Phys. Rev. A **30**, 468 (1984).
[10] B. d'Etat, J. Grumberg, E. Leboucher, H. Nguyen, and A. Poquerusse, J. Phys. B **20**, 1733 (1984).
[11] V. P. Gavrilenko, I. M. Gaisinsky, Ya O. Ispolatov, and E. A. Oks, in *Spectral Line Shapes,* edited by J. Szudy (Ossolineum Publishing House, Warsaw, 1989) Vol. 5, p. 818.
[12] Le Quang Rang and D. Voslamber, J. Phys. B **8**, 331 (1975).
[13] S. J. Rose, J. Phys. (Paris) Colloq. **44**, C8-159 (1983).
[14] B. d'Etat, Thesis, Doctorat d'état, Université Pierre et Marie Curie, Paris, 1987.
[15] D. R. Bates and R. H. G. Reid, Adv. At. Mol. Phys. **4**, 13 (1968).
[16] W. B. Brown and E. Steiner, J. Chem. Phys. **44**, 3934 (1966).
[17] G. V. Sholin, Opt. Spectrosc. **26**, 489 (1969).
[18] R. J. Damburg and R. K. H. Propin, J. Phys. B **1**, 681 (1968).
[19] S. Cooley, Math. Comput. **XV**, 363 (1961).
[20] M. M. Madsen and J. M. Peek, At. Data **2**, 171 (1971).
[21] H. R. Griem, J. Phys. (Paris) Colloq. **49**, C1 (1988); Phys. Rev. A **38**, 2943 (1988).
[22] J. C. Weisheit and E. L. Pollock, in *Spectral Line Shapes,* edited by B. Wende (de Gruyter, Berlin, 1981), Vol. 1, p. 433.